New Phytologist

Research

Elemental mapping using PIXE shows the main pathway of nickel movement is principally symplastic within the fruit of the hyperaccumulator *Stackhousia tryonii*

Naveen P. Bhatia[1], Ivo Orlic[2], Rainer Siegele[2], Nanjappa Ashwath[1], Alan J. M. Baker[3] and Kerry B. Walsh[1]

[1]Primary Industries Research Centre, School of Biological and Environmental Sciences, Central Queensland University, Rockhampton, Qld 4702, Australia; [2]Physics Division, Australian Nuclear Science and Technology Organisation (ANSTO), Lucas Heights, NSW 2234, Australia; [3]School of Botany, The University of Melbourne, Victoria 3010, Australia

Author for correspondence:
Naveen P. Bhatia
Tel: +61 74923 2316
Fax: +61 74930 9255
Email: n.bhatia@cqu.edu.au

Received: *25 May 2003*
Accepted: *30 July 2003*

doi: 10.1046/j.1469-8137.2003.00912.x

Summary

• Metal concentrations within reproductive tissues of metallophytes are rarely reported. Here, the spatial distribution of nickel (Ni) within the fruits (seeds) of the Ni hyperaccumulator *Stackhousia tryonii* was investigated.

• Two microanalytical techniques, energy dispersive x-ray spectrometry (EDXS) and nuclear microprobe (micro-proton-induced x-ray emission spectrometry; micro-PIXE) were employed for qualitative and quantitative assessment, respectively, of localized Ni, within the fruits of *S. tryonii*. The results were compared with quantitative analysis made using inductively coupled plasma-optical emission spectrometry (ICP-OES).

• Nickel analysis made using micro-PIXE was consistent with bulk (ICP-OES) analysis (at 1800 μg g^{-1} d. wt), however, a beam resolution of approx. 2×2 μm^2 allowed tissue localization. Nickel was partitioned to the fruit wall (pericarp) (4433 μg g^{-1}), while endospermic and cotyledonary tissues possessed little Ni (309 and 182 μg g^{-1} d. wt, respectively).

• This distribution is consistent with the interpretation that principal pathway of Ni movement within the fruit is symplastic rather than apoplastic (as the filial generation lacks symplastic connection with the parent).

Key words: elemental mapping, metal hyperaccumulation, nickel (Ni), nuclear microprobe analysis, micro-PIXE, quantitative imaging, spot analysis, x-ray analysis.

Abbreviations

ANSTO, Australian Nuclear Science and Technology Organisation; ICP-OES, inductively coupled plasma-optical emission spectrometry; micro-PIXE, micro-proton-induced x-ray emission spectrometry; NIST-SRM, National Institute of Standards and Technology-Standard Reference Material; OM_DAQ, Oxford Microprobe Data Acquisition System; RBS, Rutherford Backscattering Spectrometry; SEM-EDXS, scanning electron microscope-energy dispersive x-ray spectrometry.

© *New Phytologist* (2003) **160**: 479–488

Introduction

Heavy metal tolerance is the ability of a plant to grow in a heavy metal-enriched substrate that is toxic to other related plants (Macnair *et al.*, 2000). Metal accumulating plants are tolerant species (Pollard *et al.*, 2002) that can concentrate metal(s) in their above-ground tissues to levels far exceeding the concentration of metals present in the soil or in the

Table 1 Review of application of microanalytical techniques for localization of metal elements within fruit (seed) of metal-tolerant and hyperaccumulating plant species

Plant species (Family)	Metal accumulated	Metal-tolerant (T)/ hyperaccumulator (A)	Technique	Fruit/seed part examined	Elevated levels of metal	Reference
Senecio coronatus (Thunb.) Harv. (Asteraceae)	Ni	A	micro-PIXE	– sectioned, whole (dry) fruit	'in the part covering radicle and in the radicle itself'	Przybylowicz *et al*. (1995)
Silene vulgaris (Moench.) Garke (Caryophyllaceae)	Zn	T	micro-PIXE	– outer testa (intact seed) – across longitudinal section	homogeneously distributed (barring embryonic tissues) across the longitudinally cut seed	Mesjasz-Przybylowicz *et al*. (1999)
Biscutella laevigata L. (Brassicaceae)	Zn	A	micro-PIXE	– whole seed (removed from silicula)	endosperm	Mesjasz-Przybylowicz *et al*. (2001a)
Thlaspi pindicum Hausskn. (Brassicaceae)	Ni	A	SEM-EDXS	– outer testa (whole seed) – across longitudinal section	– micropylar area in epidermis of cotyledons – embryo epidermis	Psaras & Manetas (2001)

nonaccumulating species growing nearby (Baker & Brooks, 1989). The term nickel hyperaccumulator (Reeves, 1992) refers to a plant with nickel concentrations exceeding 1000 μg g^{-1} (0.1%) in its dry matter of any above-ground tissue. Metal concentrations in hyperaccumulators follow the general trend: leaf > stem > root (Homer *et al*., 1991; Mesjasz-Przybylowicz *et al*., 1994, 2001b; Gabbrielli *et al*., 1997; Robinson *et al*., 2003). However, some systems (notably, latex of *Sebertia acuminata*) have been reported (Jaffré *et al*., 1976) to contain exceptionally high levels of Ni (> 25%; d. wt basis).

Most metal localization studies have focused on leaf and stem tissues with few reported studies on metal content of fruits/seeds (Table 1). Metal contents have generally been noted to be lower in fruit/seed than in the vegetative plant body. Indeed, exclusion of metals from embryonic tissues may maintain the high reproductive success of hyperaccumulating plants on metal-enriched soils, as suggested for metal-tolerant species by Mesjasz-Przybylowicz *et al*. (1999) and Ernst *et al*. (1992).

For example, in the Ni hyperaccumulator *Alyssum heldreichii*, seeds contained approx. 1900 μg g^{-1} Ni (d. wt basis), compared to approx. 11890–14070, 7190–17060 and 4330–9150 μg g^{-1} in leaf, stem and root tissues, respectively (Morrison, 1980). In another Ni hyperaccumulator *A. troodii*, Ni levels in leaf, stem and root tissues were reported at 10084, 8540 and 1959 μg g^{-1} d. wt, respectively, while seeds contained approx. 1900 μg Ni g^{-1} d. wt (Homer *et al*., 1991). Severne (1974) noted relatively higher Ni levels in the flowers of Ni hyperaccumulator *Hybanthus floribundus* (5003 μg g^{-1}), while leaves and seeds possessed 3665 and 2000 μg g^{-1} Ni, respectively. Similarly, in Ni hyperaccumulator *A. bertolonii*, Gabbrielli *et al*. (1997) found 9908, 1684 and 1193 μg Ni g^{-1} d. wt, respectively, in leaves, stems and roots, while flowers and seeds contained relatively higher Ni levels at 7939 and 3283 μg Ni g^{-1} d. wt, respectively. Similar heavy metal accumulation patterns have been reported in the zinc (Zn) hyperaccumulator *Thlaspi caerulescens*, which possessed only 523 μg g^{-1} Zn in seeds and 10461 and 4903 μg g^{-1} (d. wt) Zn in leaf and root tissues, respectively (Ernst, 1996). In addition, Ernst *et al*. (2000) noted very low Fe, Mn, Zn and Cu accumulations in whole seeds of Zn- and Cd-resistant ecotypes of *Silene vulgaris* grown on orogenic soils, in contrast with that in vegetative parts.

The above gross distribution patterns have been based on chemical analysis of tissues using atomic absorption spectrometry or ICP-based techniques. Localization at a tissue/cellular level within the fruit and seed requires employment of microanalytical techniques. Energy dispersive x-ray spectrometry (EDXS) has been employed for cellular localization and semiquantitative analysis of a variety of metals within seed, leaf, stem and root tissues of several metal hyperaccumulating plants (Küpper *et al*., 2000, 2001; Psaras & Manetas, 2001; Lombi *et al*., 2002; Sahi *et al*., 2002; Robinson *et al*., 2003). An alternative technique, micro-proton-induced x-ray emission spectrometry (micro-PIXE) is widely regarded as a reliable microanalytical tool for quantitative localization of metals within plant tissues (Krämer *et al*., 1997; Przybylowicz *et al*., 1999, 1997; Mesjasz-Przybylowicz *et al*., 2001a, 2001b, 1999, 1997; Mesjasz-Przybylowicz & Przybylowicz, 2002), but is, however, limited in its application by accessibility to a proton beam facility. This technology is available

to the Australian scientific community through the agency of the Australian Nuclear Science and Technology Organisation (ANSTO).

Our literature searches revealed only four reports of metal localization within fruit/seed tissues of metal tolerant/hyperaccumulating plants in which micro-PIXE (three reports) and SEM-EDXS (one report) were employed as analytical tools (Table 1). No study has considered distribution of heavy metals in the fruit/seed of *S. tryonii*. All the micro-PIXE studies on spatial distribution and localization of various metal elements within fruit/seed of metal-tolerant/hyperaccumulating plants were performed using the nuclear microprobe facility (operated with 3.0 MeV protons) at the National Accelerator Centre (NAC), Faure, South Africa (Table 1). In most of these studies, the beam spot size and beam current employed were approx. 3 μm^2 and 100–500 pA, respectively. Two complementary techniques – PIXE and proton backscattering (BS) – were employed for point analysis and/or dynamic elemental mapping in the NAC studies.

Published reports are not consistent with respect to the distribution of heavy metals within the fruit/seed. For example, in the Ni higher Ni concentrations in the rudimentary endosperm (14000 $\mu g\ g^{-1}$) and pulp (inferred as mesocarp; 8000 $\mu g\ g^{-1}$), while cotyledons (5000 $\mu g\ g^{-1}$), fruit peel (inferred as exocarp; 4000 $\mu g\ g^{-1}$) and seed peel (inferred as testa; 1000 $\mu g\ g^{-1}$) possessed comparatively lower Ni concentrations. In a SEM-EDXS study of Ni localization in whole seeds of the hyperaccumulator *Thlaspi pindicum*, Psaras & Manetas (2001) reported that Ni concentrations were 15-times higher within the micropylar area, relative to the rest of the testa. In addition, Ni was detected in the epidermis of longitudinal sections of cotyledons and embryo but not in other embryonic tissues. Przybylowicz *et al.* (1995) employed micro-PIXE in a study of sectioned fruit of *Senecio coronatus* and noted elevated Ni levels in the seed radicle (relative to the receptacle, embryo, seed coat and pericarp). Mesjasz-Przybylowicz *et al.* (1999) also employed similar techniques in studies of seeds of the Zn-tolerant *Silene vulgaris* and reported that Zn was excluded from embryonic tissues, but relatively homogeneously distributed throughout other seed tissues. In a study of elemental distribution in another Zn-tolerant species, *Biscutella laevigata* L., Mesjasz-Przybylowicz *et al.* (2001b) reported elevated levels of Zn (414 $\mu g\ g^{-1}$ d. wt) within endospermic tissues, while the pericarp, hilum area, testa, cotyledons and hypocotyls contained, respectively, 130, 134, 44, 61 and 87 $\mu g\ g^{-1}$ of Zn.

Stackhousia tryonii Bailey (family Stackhousiaceae) is a rare, understorey, perennial, Ni-hyperaccumulating herb. It is endemic to serpentinite outcrops of Central Queensland (Australia) and has been reported (Batianoff *et al.*, 1990; Batianoff & Specht, 1992) to hyperaccumulate Ni in both leaves and stems to levels up to 41 300 and 7800 $\mu g\ g^{-1}$ d. wt, respectively. It usually flowers after seasonal rains, and produces a large number of fruits. The fruit is a *schizocarp*, breaking at maturity into three single-seeded units, each about 2 mm long, consisting of a seed within a carpel. Mature (dry) seeds have very poor germination, with only 5–10% germinating readily after picking (N. P. Bhatia, unpublished).

Localization of Ni using SEM-EDXS in vegetative tissues of *S. tryonii* has been reported in a few studies (Bidwell, 2000; Noell & Morris, 1996, 1997). Traditional destructive analysis (ICP) has been used in one report of Ni hyperaccumulation within reproductive tissues of *S. tryonii*. Batianoff *et al.* (1990) reported relatively high concentrations of Ni (8410 $\mu g\ g^{-1}$) in a flower specimen of *S. tryonii* collected from Mt Wheeler-Bondoola (Central Queensland) and growing in a soil containing 1010 $\mu g\ g^{-1}$ (total) Ni.

To the best of our knowledge, there are no published reports on the localization of Ni within fruits of *S. tryonii*. In the present study, we have employed micro-PIXE and SEM-EDXS techniques as analytical tools to investigate Ni localization within fruits of *S. tryonii*.

Materials and Methods

Plant material

Mature (dry) fruits (*c.* 6% moisture content) of *S. tryonii* were collected from healthy plants growing in the wild on serpentine soil near Eden Bann (23°05.72′S, 150°16.41′E; about 42 km north-west of Rockhampton, Queensland, Australia). Fruits were not washed before analysis. Approx. 2 g of fruits were collected, from 50 branches of five adjacent plants, for analysis by inductively coupled plasma-optical emission spectrometry (ICP-OES). Fruits were obtained from five adjacent plants (considered as replicates) for EDXS and micro-PIXE studies.

Sample preparation

Bulk (ICP-OES) analysis A subsample (0.8 g) of fruit was digested in nitric acid (70%; v/v), and the digest analysed by ICP-OES using laboratory facilities at Incitec Ltd, Brisbane, Australia.

Specimen preparation The general technique of Przybylowicz *et al.* (1999) was followed with slight modification for micro-PIXE work. Support films for the specimens were prepared by dissolving Formvar 15/95 resin (ProSciTech, Queensland, Australia) in 2% ethylene dichloride. Drops of the Formvar solution were spread on distilled water. On drying, the film floating on the water surface was picked up across 5 mm diameter holes made on aluminium strips (thickness 300 μm). In this study, air-dried fruits (*c.* 6% moisture) were used. For future work, use of freeze-dried material is recommended (to avoid sample shrinkage; see Results). Fruits were cut, under a stereo-microscope, into two (either transversely or longitudinally)

using a sharp razor blade. The fruit halves were individually placed in the centre of the Formvar film resting across the hole. A second film was picked up with a 25-mm eye-loop (made of thin steel wire) and placed over the specimen. Thus, the specimens were sandwiched between two films. The sandwiched specimens were further air-dried for 10–15 min. The aluminium strips were glued, using double-sided carbon tape, to an aluminium holder, standard for the ANSTO microprobe facility. The specimens were photographed under light microscope to allow for easy identification and location of features within specimens during irradiation. Thereafter specimens were introduced through a vacuum lock into the proton beam of the micro-PIXE set up.

For SEM-EDXS analysis, sectioned fruit specimens were glued onto standard aluminium stubs using double-sided carbon tape.

Instrumentation and analysis

SEM-EDXS study X-ray microanalysis of prepared specimens was performed with a JEOL JSM-5300 LV scanning electron microscope (JEOL USA Inc., MA, USA) attached to a Link PentaFET system (Oxford Instruments, Oxford, UK) interfaced with Link eXII Analysis software. X-rays were detected by a Si(Li) detector (Oxford Instruments, Oxford, UK) with a thin beryllium window. The microscope was operated at an accelerating voltage of 15 kV with a collection time of 100 s. Working distance was 15 mm and stage-tilt was adjusted to obtain a take-off angle of 40°. The SEM-EDXS set up was calibrated using a cobalt reference standard (Astimex Scientific Ltd, Toronto, Canada).

Elemental composition was obtained by processing EDX spectra and images with a Link eXII Analysis. Following EDXS, specimens were gold coated for 10 min using a Bio-Rad Polaron SC515 SEM system (Fisons Instruments, East Sussex, UK), then returned to the SEM and secondary electron images acquired.

Micro-PIXE study A 10-MV Tandem accelerator at ANSTO (Australian Nuclear Science and Technology Organisation) was used (Siegele *et al.*, 1999) to provide a 3 MeV proton beam for the nuclear microprobe analyses. For point analysis and elemental mapping, both PIXE and proton backscattering (BS) were employed simultaneously. A high purity Ge X-ray detector (Canberra, USA) with an active area of 100 mm^2 and 25 μm beryllium window, positioned 30 mm from the target at an angle of 135°, was used to acquire PIXE spectra. The distance between sample and detector was adjustable (between 20 and 100 mm), such that a maximum solid angle of 250 msr was provided. A proton beam current of 200–1000 pA was used with a minimum beam spot size of 2 μm^2. The PIXE count rate was kept below 1000 counts s^{-1} in order to avoid pulse pile-up. The proton beam was scanned over sample areas of between 0.4×0.4 mm^2 and 2.5×2.5 mm^2. To achieve satisfactory counting statistics, samples were typically irradiated with a total charge between 0.5 and 3 μC. Signals from the detectors were recorded using OM_DAQ (Oxford Microprobe Data Acquisition System, Oxford Microbeams Ltd, Oxford) (Grime & Dawson, 1995). The OM_DAQ also controls beam scanning and allows the accumulation of elemental maps, line scans and point analyses (Krämer *et al.*, 1997). The PIXE set up was calibrated using a NIST Standard Reference Material (NIST-SRM #278; Obsidian rock) containing 3.6 ± 0.3 μg g^{-1} Ni. The Backscattering analysis (BS) was calibrated using thin Perspex of known thickness and composition. Following micro-PIXE analysis, specimens were gold coated and photomicrographs obtained as described under SEM-EDXS study.

The PIXE spectra were analysed using GeoPIXE II software. This program allows extraction of PIXE elemental maps from the accumulated data using Dynamic Analysis (Ryan, 2001), which are overlap-resolved and background-subtracted. Using the 'region selection' mode (Dynamic Analysis), various regions (pericarp, endosperm, cotyledons) from the images (reproduced on computer screen from data accumulated by OM_DAQ) of transversely cut fruits were selected for spot and point analyses. Spot analysis within cotyledons and endosperm was attempted by encircling (circle diameter between 2900 and 5400 μm^2) representative areas within three replicate seeds. Within the pericarp, which encases the endosperm, spot analysis was carried out on rectangular-shaped 'boxes' of fixed area (4576×693 μm).

Tissue density within the seed specimens is not homogeneous. The composition of the sample matrix was assumed to be comparable to cellulose (following the procedure of Pineda & Peisach, 1988), and RBS (Rutherford Backscattering Spectrometry) spectra from respective regions were approximated to that of cellulose (using NUSDAN software), allowing adjustment of area density calculation for a specific region of interest and consequently final adjustment of elemental concentrations.

Results

SEM-EDXS analysis

The fruit of *S. tryonii* is a *schizocarp*, possessing a dry and indehiscent pericarp that surrounds the seed. The seed consists of a seed coat, enclosing the endosperm and cotyledons (Fig. 2a,e). The embryonic axis was not distinguishable in the fruits examined, suggesting that the embryo is poorly developed at fruit maturity. Visibly mature (dry) fruits were collected, however, there was a variable amount of separation between pericarp and endosperm/cotyledon amongst replicate fruits. Figure 2(a) is an example of a fruit with little separation. This suggests variation in moisture content or maturity of *S. tryonii* fruits. The testa was also closely adhering to the endosperm (Fig. 2a).

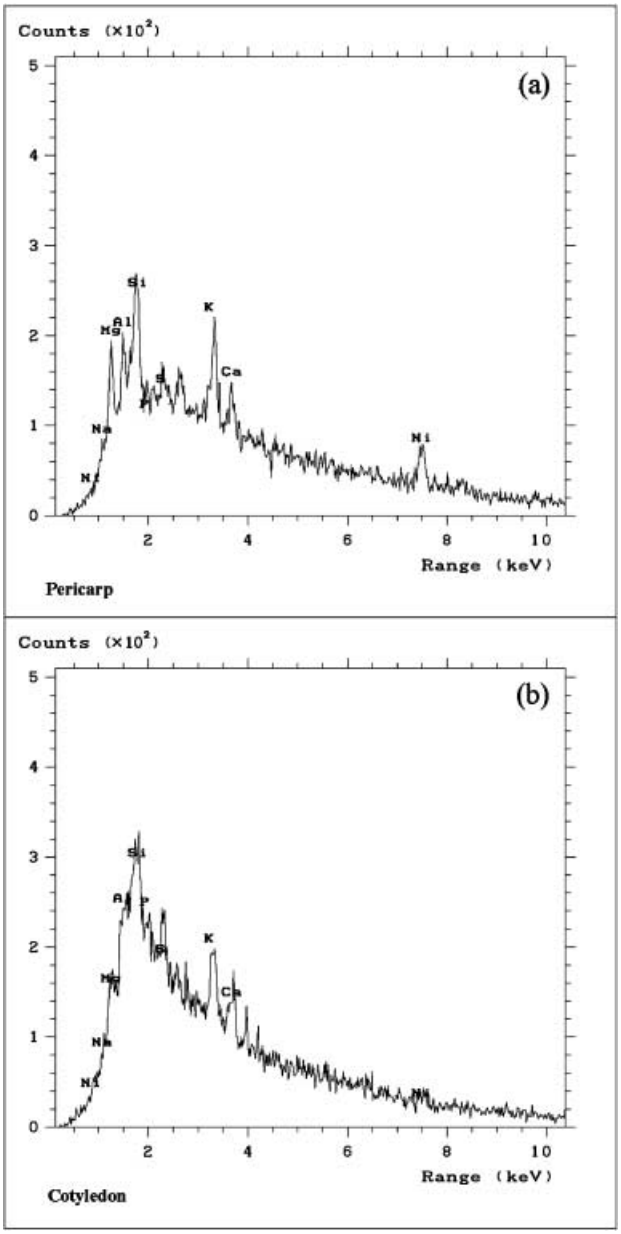


Fig. 1 Typical energy-dispersive x-ray spectra of pericarp (a) and cotyledon (b) of the fruit of *Stackhousia tryonii*. Fruits accumulated potassium, calcium and nickel in pericarp, and phosphorus, sulphur, potassium and calcium in cotyledons. Higher peaks of aluminium and silica are attributed to possible contamination of exposed surface while sectioning, as unwashed fruits were used in the present study.

The EDXS assessment of *S. tryonii* fruit revealed the presence of elevated concentrations of Ni in the pericarp (Fig. 1a) with low amounts of Ni in the central cotyledonary tissues (Fig. 1b).

Micro-PIXE analysis Micro-PIXE analysis caused damage to the specimens, with separation of the pericarp, testa and endosperm (Fig. 2e). This shrinkage was presumably due to the high thermal load of the proton beam and to desiccation under vacuum. The fruits contained about 6% moisture and since the analysis was carried out in vacuum, any free water in vacuum would therefore have been lost from the specimen. However, remaining water (chemically bound; if any) was sufficiently low and did not affect the analysis of the specimens. The loss of water would change the matrix composition slightly but this was accounted for by iterative procedures on the matrix stopping power.

In the bulk (ICP-OES) analysis of *S. tryonii* fruits, concentrations of various elements followed the order: K > Ni > S > Ca > Fe > Zn > Mn > Cu. The concentrations of micronutrient elements (Fe, Zn, Mn, Cu) obtained by micro-PIXE analysis were slightly higher than those obtained by bulk analysis (Table 2). For Ni, the results of micro-PIXE analysis of whole fruit sections (assessed of a seed cross section) were similar to those of bulk (ICP-OES) analysis (i.e. 1400 μg g^{-1} and 1800 μg g^{-1} Ni, respectively). However, this comparison assumes that the examined central section was proportionately representative of the whole fruit. On a weight basis, the pericarp : endosperm plus cotyledons ratio was 1.27 : 1.

Elemental distribution amongst tissues (pericarp, endosperm, cotyledons) was not uniform (Table 2; Figs 1, 2b,c,d and 3). The concentration of Ni was the highest in the pericarp (4433 μg g^{-1}), while endosperm and cotyledons contained comparatively low Ni at 309 and 182 μg g^{-1}, respectively. Given that a 1.27 : 1 ratio (weight to weight basis) existed for pericarp : endosperm plus cotyledons, the total Ni concentration within the fruit (adjusted for pericarp:seed weight) was calculated to be 2696 μg g^{-1}. This estimate is also in general agreement with values obtained by bulk (ICP-OES) analysis.

There was no evidence of localization of Ni on the fruit surface (i.e. superficial contamination from wind-blown dust and soil particles). Nickel was localized within cell layers within the outer-to-middle pericarp (Figs 2f and 3). However, Ni concentration within this layer was not uniform. In consequence, Ni concentration varied greatly, as evidenced by the higher standard error (6280 ± 2062 μg Ni g^{-1}, $n = 5$; Table 3). Ca was predominantly localized along the outer periphery of the endosperm, bordering the testa/pericarp (Figs 2b and 3). The concentration of Ca was similar in endosperm (1467 μg g^{-1}) and pericarp (1333 μg g^{-1}) (Fig. 2b, Table 2). By contrast, K concentration increased inwards, from the outer tissues (pericarp; 996 μg g^{-1}) to the central tissues (cotyledons; 5567 μg g^{-1}) (Figs 2c and 3). Sulphur (S) concentration was similar in the endosperm and cotyledons (2433 and 2200 μg g^{-1}, respectively), and very low in the pericarp (Table 2). The concentration of Zn and Mn was largely uniform across fruit tissues, whereas maximum concentrations of Fe and Cu were found in the pericarp (Table 2).

'Spot' counts were made within each tissue in order to quantify variability within a tissue and amongst the replicates (Table 3). Variation in Ni concentration amongst the replicates was small, relative to the difference amongst tissues (i.e. pericarp, endosperm, cotyledons).

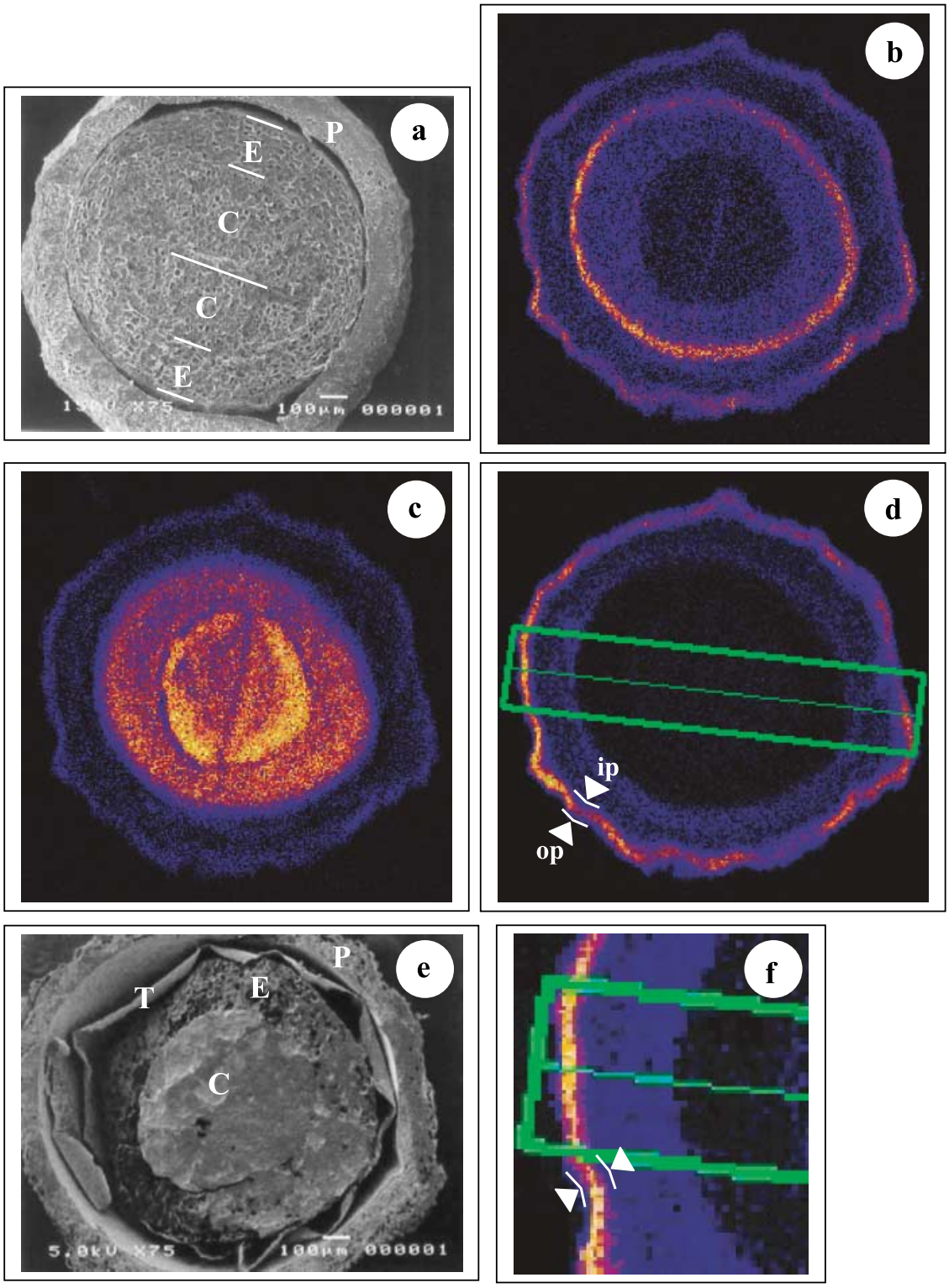


Fig. 2 Typical secondary electron image (SEI) of a fruit before irradiation with proton beam (a), and distribution pattern of calcium (b), potassium (c) and nickel (d) within a transversely-cut fruit of *Stackhousia tryonii* (micro-PIXE analysis). (e) SEI of the same fruit following proton beam irradiation. Traverse on nickel image relates to quantitative point analysis across fruit shown in Fig. 3. (f) High magnification of a part of (d). Labels 'E', 'C', 'P' and 'T' in images (a) and (e) represent endosperm, cotyledons, pericarp and testa, respectively (white lines separate endospermic tissues from cotyledonary tissues). op, outer pericarp; ip, inner pericarp.

Table 2 Average concentration of elements within fruits of *Stackhousia tryonii* as estimated using ICP-OES analysis of a bulk fruit sample and micro-PIXE analysis for three fruits

	Concentration (μg g^{-1} dry mass)				
	ICP-OES	Micro-PIXE			
Element	Bulk	Whole section	Pericarp	Endosperm	Cotyledons
K	2750	3000 ± 58	996 ± 104	4333 ± 338	5567 ± 669
Ni	**1800**	**1400 ± 58**	**4433 ± 669**	**309 ± 38**	**182 ± 47**
S	1450	1114 ± 139	< 15	2433 ± 546	2200 ± 346
Ca	950	1067 ± 117	1333 ± 33	1467 ± 167	333 ± 82
Fe	37	90 ± 8	180 ± 23	59 ± 8	68 ± 14
Zn	28	55 ± 10	53 ± 8	71 ± 15	68 ± 16
Mn	24	30 ± 6	38 ± 6	28 ± 5	38 ± 7
Cu	8	18 ± 3	49 ± 8	13 ± 6	1 ± 1

Values are mean ± SE for whole section, pericarp, endosperm and cotyledons. Micro-PIXE results obtained using the 'region selection' mode o Dynamic Analysis. Ni results are shown in bold type. ICP-OES, inductively coupled plasma-optical emission spectrometry; micro-PIXE, micro-prot induced x-ray emission spectrometry.

Table 3 Average concentration of various elements within fruits of *Stackhousia tryonii* as determined by micro-PIXE using spot analysis

				Concentration (μg g^{-1} dry mass)		
Seed part	Replicates	Spot area (μm^2)	No. of spot measurements	Ca	K	Ni
Cotyledons	1	2917	4	526 ± 82	8500 ± 668	592 ± 102
	2	5414	5	369 ± 100	6780 ± 719	215 ± 22
	3	5423	3	671 ± 105	7333 ± 926	350 ± 7
Endosperm	1	2917	3	3967 ± 1141	7176 ± 546	444 ± 63
	2	5414	5	2280 ± 413	6420 ± 981	173 ± 18
	3	5423	2	3200 ± 800	6700 ± 1200	182 ± 5
Pericarp	1	4576 × 693	5	3840 ± 673	3360 ± 479	6280 ± 2062

Values are mean ± SE. Replicate fruits were obtained from adjacent plants. Micro-PIXE, Micro-proton-induced x-ray emission spectrometry.

Discussion

Technique choice

SEM-EDXS is a versatile technique for estimating the spatial distribution of chemical elements in cells (Zierold & Hagler, 1989), but suffers from poor quantification because of the unknown volumes of the tissues sampled. By contrast, micro-PIXE technique, using tissue sections, potentially allows quantitative analysis, but has lower spatial resolution. However, micrometer level resolution has been reported (Malmqvist, 1995).

The SEM-EDXS protocol employed in the present study was able to detect Ni in the specimen, but quantification was not possible. However, the SEM secondary electron images provide excellent anatomical detail. The micro-PIXE technique allowed Ni localization maps to be prepared with a beam resolution (pixel size) of 2 × 2 μm.

The prolonged exposure to proton beam presumably caused heating and moisture loss, resulting in tissue shrinkage. This specimen movement during analysis would degrade the effective resolution during elemental mapping.

Elemental distribution in seed

The fruits examined in the present study were mature, with a nonliving pericarp. It is therefore expected that mobile elements, such as K, will have been re-translocated from the pericarp. Nonmobile elements, such as Ca, Fe and S, are expected to remain within the pericarp. The observed patterns of distribution are consistent with this interpretation.

Ni localization within fruit and seed

Fruits were not washed to avoid redistribution (and leaching) of metals. Contamination of the fruit by Ni containing soil would have been obvious as particulate matter on the fruit surface. This was not observed. Nickel was localized in cell layers within the pericarp.

The distribution pattern for Ni noted in this study, with high concentration in the pericarp (6280 μg g^{-1}), is consistent with transport of Ni within the fruit via symplastic pathways, and a symplastic isolation of the filial generation. Presumably, a low level of apoplastic movement occurred, as some Ni was

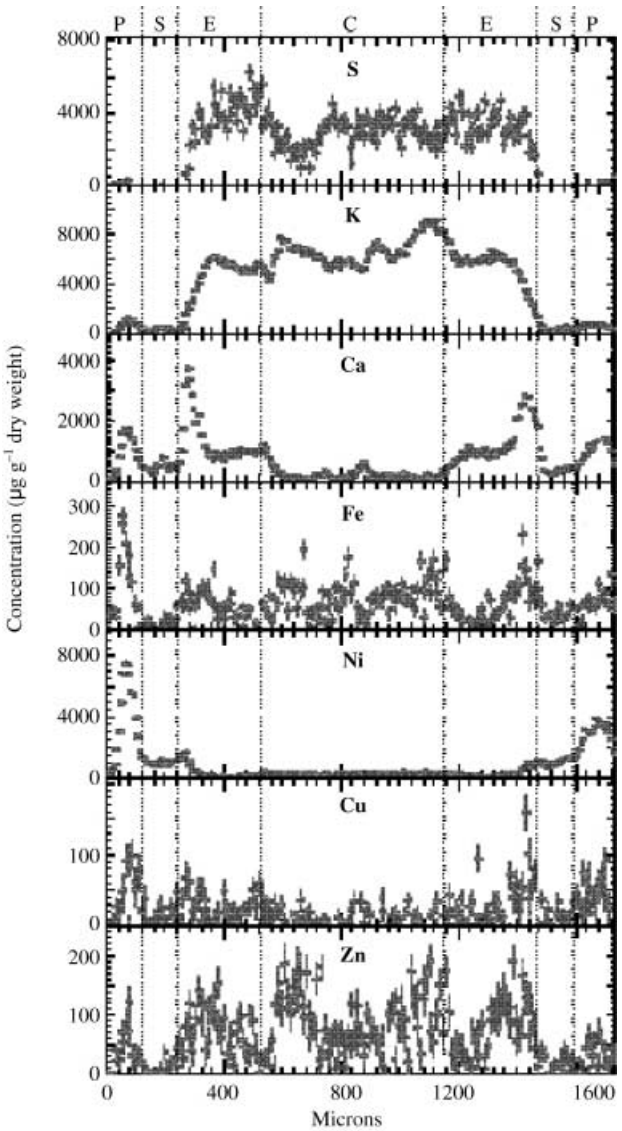


Fig. 3 Quantitative traverse point analysis across the transect outlined in Fig. 2. Letters P, S, E and C on top of the graph represent pericarp, space between pericarp and testa (viewing inner wall of pericarp), endospermic and cotyledonary areas (separated by dashed lines), respectively.

noted in the endosperm (309 μg g^{-1}) and cotyledons (182 μg g^{-1}). The megasporangium (placenta; Ernst *et al.*, 1992) and the endosperm (Mesjasz-Przybylowicz *et al.*, 2001a) have been previously suggested to act as a barrier to metal transport within seed of metal tolerant/accumulating species, preventing the entry of toxic elements into embryonic tissues.

It is difficult to envisage a precise physiological explanation for some reported distribution patterns. The pathways of solute transport to reproductive tissues are considered to be conservative across all angiosperm species, and are well described in a review by Patrick (1997). In summary, fruit growth is supported by the supply of organic material through the phloem. The mass movement of phloem fluids may also incidentally deliver other materials (e.g. certain heavy metals) to the fruit. When phloem-supplied water is in excess of fruit transpiration requirements, it will return to the stem via the xylem of peduncle. Presumably, some heavy metals will be recirculated to the plant body via this pathway. Within fruit, phloem-supplied materials may be distributed symplastically within the fruit wall (pericarp), but symplastic discontinuities exist at the pericarp-endosperm and endosperm-cotyledon/embryo interfaces. Phloem-supplied material must move apoplastically across these interfaces to the progeny (endosperm, cotyledons or embryo). In many cases, the cell layers involved at this interface are composed of transfer cells. Symplastic movement is possible within the endosperm and cotyledons/embryo, but there is a symplastic discontinuity between the endosperm and cotyledons/embryo. Therefore, the distribution pattern for Ni noted in this study, with high concentration in the pericarp, appears consistent with transport via symplastic pathways, and with relatively low concentrations of Ni in the filial generation (i.e. embryo and endosperm).

Other literature reports of heavy metal accumulation in seed (see Introduction) are not consistent with the above physiological explanation. These reports require verification and, potentially, consideration of other mechanisms.

Postulated roles for Ni in fruit: germination and antiherbivory

The field-collected fruits of *S. tryonii* had very poor germination, even in favourable media (N. P. Bhatia, unpublished). This poor germination might be linked to the high content of metals within fruit/seed, as suggested for *Silene vulgaris* by Ernst & Nelissen (2000). It is possible that Ni is re-distributed from the pericarp via apoplastic pathways during imbibition and germination.

However, Ni solution concentrations of > 5000 μg cm^{-3} were required to inhibit germination of both Ni hyperaccumulator (*Alyssum troodii* Boiss) and nonhyperaccumulator (*Aurinia saxatilis* L.) species (Homer *et al.*, 1991). In the case of *S. tryonii*, the average fruit (pericarp and seed) contains 1.57 μg Ni (average weight of pericarp = 0.87 mg; Ni bulk analysis, 1800 μg g^{-1}, see Table 2). Fruit weight increases by 38% during imbibition. Thus, a fruit of weight 1.56 mg takes up 0.59 mg (59 μl) of water during imbibition. Dissolution of the seed Ni content (1.57 μg Ni) into this volume of water results in a concentration of only 27 μg cm^{-3}. Further dilution is expected through diffusion into soil water. Thus, unless *S. tryonii* seed is particularly sensitive to Ni, low germination is unlikely to be related to the Ni content of the pericarp. Preliminary trials indicated that seed germination in *S. tryonii* was not inhibited by up to 100 μg cm^{-3} Ni (data not shown). We suggest that low germination values in *S. tryonii* may more likely be related to embryo immaturity.

The hyperaccumulation trait has been suggested to function as a defence against herbivory and pathogen attack (Boyd & Martens, 1992). The localization of Ni in the plant epidermis may be of significance as the epidermis is the first line of plant defence against insect herbivory (Schoonhoven *et al.*, 1998). The high Ni levels (1800 μg g^{-1}) in *S. tryonii* pericarp might be sufficient to deter herbivores, and hence maintain a higher rate of healthy fruit fall on the floor that will germinate after seasonal rains.

Acknowledgements

A merit scholarship (UPRA) to NPB by the Central Queensland University and financial assistance (Grant no. 450; 02/001P) for the present work by the Australian Institute of Nuclear Science and Engineering (AINSE) is gratefully acknowledged. We also acknowledge helpful discussions by Prof J.N.A. Lott (McMaster University, Canada) on patterns of elemental distribution within seed, critical reviewing of the manuscript by Dr Ani Nkang (University of Calabar, Nigeria), the technical assistance of Mr V. McCafferty with SEM, and the assistance of Queensland Parks and Wildlife Services (Central Region) for granting a scientific permit to collect *S. tryonii* material from its natural habitat.

References

Baker AJM, Brooks RR. 1989. Terrestrial higher plants which hyperaccumulate metallic elements – a review of their distribution, ecology and phytochemistry. *Biorecovery* **1**: 81–126.

Batianoff GN, Reeve RD, Specht RL. 1990. *Stackhousia tryonii* Bailey: a nickel-accumulating serpentine-endemic species of Central Queensland. *Australian Journal of Botany* **38**: 121–130.

Batianoff GN, Specht RL. 1992. Queensland (Australia) serpentinite vegetation. In: Baker AJM, Proctor J, Reeves RD, eds. *The vegetation of ultramafic (serpentine) soils. Proceedings of the First International Conference on Serpentine Ecology*. Andover, UK: Intercept Ltd, 109–128.

Bidwell SD. 2000. *Hyperaccumulation of metals in Australian native plants*. PhD thesis, The University of Melbourne, Australia.

Boyd RS, Martens SN. 1992. The *raison d'Être* for metal hyperaccumulation by plants. In: Baker AJM, Proctor J, Reeves RD, eds. *The vegetation of ultramafic (serpentine) soils. Proceedings of the First International Conference on Serpentine Ecology*. Andover, UK: Intercept Ltd, 279–290.

Ernst WHO, Nelissen HJM. 2000. Life cycle phases of a zinc- and cadmium-resistant ecotype of *Silene vulgaris* in risk assessment of polymetallic mine soils. *Environmental Pollution* **107**: 329–338.

Ernst WHO, Nelissen HJM, Ten Bookum WM. 2000. Combination toxicology of metal-enriched soils: physiological responses of a Zn- and Cd-resistant ecotype of *Silene vulgaris* on polymetallic soils. *Environmental and Experimental Botany* **43**: 55–71.

Ernst WHO, Verkleij JAC, Schat H. 1992. Metal tolerance in plants. *Acta Botanica Neerlandica* **41**: 229–248.

Ernst WHO. 1996. Bioavailability of heavy metals and decontamination of soils by plants. *Applied Geochemistry* **11**: 163–167.

Gabbrielli R, Gremigni P, Bonzi Morassi L, Pandolfini T, Medeghini P. 1997. Some aspects of Ni tolerance in *Alyssum bertolonii* Desv. strategies of metal distribution and accumulation. In: Jaffré T, Reeves RD, Becquer T, eds. *The ecology of ultramafic and metalliferous areas. Proceedings of the Second International Conference on Serpentine Ecology, Nouméa*. Nouméa, New Caledonia: ORSTOM, 225–227.

Grime GW, Dawson M. 1995. Recent developments in data acquisition and processing on the Oxford scanning proton microprobe. *Nuclear Instruments and Methods in Physics Research Section B–Beam Interactions with Materials and Atoms* **104**: 107–113.

Homer FA, Morrison RS, Brooks RR, Clemens J, Reeves RD. 1991. Comparative studies of nickel, cobalt and copper uptake by some nickel hyperaccumulators of the genus *Alyssum*. *Plant and Soil* **138**: 195–205.

Jaffré T, Brooks RR, Lee V, Reeves RD. 1976. *Sebertia acuminata*: a hyperaccumulator of nickel from New Caledonia. *Science* **193**: 579–580.

Krämer U, Grime GW, Smith JAC, Hawes CR, Baker AJM. 1997. Micro-PIXE as a technique for studying nickel localization in leaves of the hyperaccumulator plant *Alyssum lesbiacum*. *Nuclear Instruments and Methods in Physics Research Section B–Beam Interactions with Materials and Atoms* **130**: 346–350.

Küpper H, Lombi E, Zhao FJ, McGrath SP. 2000. Cellular compartmentation of cadmium and zinc in relation to other elements in the hyperaccumulator *Arabidopsis halleri*. *Planta* **212**: 75–84.

Küpper H, Lombi E, Zhao FJ, Wieshammer G, McGrath SP. 2001. Cellular compartmentation of nickel in the hyperaccumulators *Alyssum lesbiacum*, *Alyssum bertolonii* and *Thlaspi goesingense*. *Journal of Experimental Botany* **52**: 2291–2300.

Lombi E, Zhao FJ, Fuhrmann M, Ma LQ, McGrath SP. 2002. Arsenic distribution and speciation in the fronds of the hyperaccumulator *Pteris vittata*. *New Phytologist* **156**: 195–203.

Macnair MR, Tilstone GH, Smith SE. 2000. The genetics of metal tolerance and accumulation in higher plants. In: Terry N, Bañuelos G, eds. *Phytoremediation of contaminated soil and water*. Boca Raton, FL, USA: CRC Press, 235–250.

Malmqvist KG. 1995. Biological and Medical Application. In: Johansson SAE, Campbell JL, Malmqvist KG, eds. *Particle-induced x-ray emission spectrometry. Chemical Analysis Series, Vol. 133*. New York, USA: John Wiley & Sons, Inc, 167–236.

Mesjasz-Przybylowicz J, Balkwill K, Przybylowicz WJ, Annegarn HJ. 1994. Proton microprobe and X-ray fluorescence investigations of nickel distribution in serpentine flora from South Africa. *Nuclear Instruments and Methods in Physics Research Section B–Beam Interactions with Materials and Atoms* **89**: 208–212.

Mesjasz-Przybylowicz J, Grodzinska K, Przybylowicz WJ, Godzik B, Szarek-Lukaszewska G. 2001a. Nuclear microprobe studies of elemental distribution in seeds of *Biscutella laevigata* L. from zinc wastes in Olkusz, Poland. *Nuclear Instruments and Methods in Physics Research Section B–Beam Interactions with Materials and Atoms* **181**: 634–639.

Mesjasz-Przybylowicz J, Grodzinska K, Przybylowicz WJ, Godzik B, Szarek-Lukaszewska G. 1999. Micro-PIXE studies of elemental distribution in seeds of *Silene vulgaris* from a zinc dump in Olkusz. southern Poland. *Nuclear Instruments and Methods in Physics Research Section B–Beam Interactions with Materials and Atoms* **158**: 306–311.

Mesjasz-Przybylowicz J, Przybylowicz WJ. 2002. Micro-PIXE in plant sciences: present status and perspectives. *Nuclear Instruments and Methods in Physics Research Section B–Beam Interactions with Materials and Atoms* **189**: 470–481.

Mesjasz-Przybylowicz J, Przybylowicz WJ, Pineda CA. 2001b. Nuclear microprobe studies of elemental distribution in apical leaves of the Ni hyperaccumulator *Berkheya coddii*. *South African Journal of Science* **97**: 591–593.

Mesjasz-Przybylowicz J, Przybylowicz WJ, Prozesky V, Pineda CA. 1997. Quantitative micro-PIXE comparison of elemental distribution in Ni-hyperaccumulating and non-accumulating genotypes of *Senecio coronatus*. *Nuclear Instruments and Methods in Physics Research Section B–Beam Interactions with Materials and Atoms* **130**: 368–373.

Mesjasz-Przybylowicz J, Przybylowicz WJ, Rama DBK, Pineda CA. 2001c. Elemental distribution in *Senecio anomalochrous*, a Ni hyperaccumulator from South Africa. *South African Journal of Science* **97**: 593–595.

Morrison RS. 1980. *Aspects of the accumulation of cobalt, copper and nickel by plants*. PhD thesis, Massey University, New Zealand.

Noell I, Morris D. 1996. Localisation of hyperaccumulated nickel in *Stackhousia tryonii* using electron-probe microanalysis. In: Bailey GW, Corbett JM, Dimlich RVW, Michael JR, Zaluzec NJ, eds. *Proceedings of Microscopy and Microanalysis*. San Francisco, CA, USA: USA. San Francisco Press Inc, 92–93.

Noell I, Morris D. 1997. Nickel concentrations and plant defence in *Stackhousia tryonii*. In: Jaffré T, Reeves RD, Becquer T, eds. *The Ecology of Ultramafic and Metalliferous Areas. Proceedings of the Second International Conference on Serpentine Ecology, Nouméa*. Nouméa, New Caledonia: ORSTOM, 109–110.

Patrick JW. 1997. Phloem unloading: sieve element unloading and post-sieve element transport. *Annual Review of Plant Physiology and Plant Molecular Biology* **48**: 191–222.

Pineda CA, Peisach M. 1988. Matrix corrections for the determination of trace elements in thick biological samples by PIXE. *Nuclear Instruments and Methods in Physics Research Section B–Beam Interactions with Materials and Atoms* **35**: 344–348.

Pollard AJ, Powell KD, Harper FA, Smith JAC. 2002. The genetic basis of metal hyperaccumulation in plants. *Critical Reviews in Plant Sciences* **21**: 539–566.

Przybylowicz WJ, Mesjasz-Przybylowicz J, Pineda CA, Churms CL, Springhorn KA, Prozesky VM. 1999. Biological applications of the NAC nuclear microprobe. *X-Ray Spectrometry* **28**: 237–243.

Przybylowicz WJ, Mesjasz-Przybylowicz J, Prozesky VM, Pineda CA. 1997. Botanical applications in nuclear microscopy. *Nuclear Instruments and Methods in Physics Research Section B–Beam Interactions with Materials and Atoms* **130**: 335–345.

Przybylowicz WJ, Pineda CA, Prozesky VM, Mesjasz-Przybylowicz J. 1995. Investigation of Ni hyperaccumulation by true elemental imaging. *Nuclear Instruments and Methods in Physics Research Section B–Beam Interactions with Materials and Atoms* **104**: 176–181.

Psaras GK, Manetas Y. 2001. Nickel localization in seeds of the metal hyperaccumulator *Thlaspi pindicum* Hausskn. *Annals of Botany* **88**: 513–516.

Reeves RD. 1992. Hyperaccumulation of nickel by serpentine plants. In: Baker AJM, Proctor J, Reeves RD, eds. *The vegetation of ultramafic (serpentine) soils. Proceedings of the First International Conference on Serpentine Ecology*. Andover, UK: Intercept Ltd, 253–277.

Robinson BH, Lombi E, Zhao FJ, McGrath SP. 2003. Uptake and distribution of nickel and other metals in the hyperaccumulator *Berkheya coddii*. *New Phytologist* **158**: 279–285.

Ryan CG. 2001. Developments in Dynamic Analysis for quantitative PIXE true elemental imaging. *Nuclear Instruments and Methods in Physics Research Section B–Beam Interactions with Materials and Atoms* **181**: 170–179.

Sagner S, Kneer R, Wanner G, Cosson J-P, Deus-Neumann B, Zenk MH. 1998. Hyperaccumulation, complexation and distribution of nickel in *Sebertia acuminata*. *Phytochemistry* **47**: 339–347.

Sahi SV, Bryant NL, Sharma NC, Singh SR. 2002. Characterization of a lead hyperaccumulator shrub, *Sesbania drummondii*. *Environmental Science and Technology* **36**: 4676–4680.

Schoonhoven LM, Jermy T, van Loon JJA. 1998. *Insect-plant biology: from physiology to evolution*. London, UK: Chapman & Hall.

Severne BC. 1974. Nickel accumulation by *Hybanthus floribundus*. *Nature* **248**: 807–808.

Siegele R, Cohen DD, Dytlewski N. 1999. The ANSTO high energy heavy ion microprobe. *Nuclear Instruments and Methods in Physics Research Section B–Beam Interactions with Materials and Atoms* **158**: 31–38.

Zierold K, Hagler HK. 1989. *Electron probe microanalysis applications in biology and medicine*. Berlin, Germany: Springer Verlag.

About *New Phytologist*

- *New Phytologist* is owned by a non-profit-making **charitable trust** dedicated to the promotion of plant science. Regular papers, Letters, Research reviews, Rapid reports and Methods papers are encouraged. Complete information is available at **www.newphytologist.org**
- All the following are **free** – essential colour costs, 25 offprints as well as a PDF (i.e. an electronic version) for each article, online summaries and ToC alerts (go to the website and click on 'Journal online')
- You can take out a **personal subscription** to the journal for a fraction of the institutional price. Rates start at £86 in Europe/$145 in the USA & Canada for the online edition (go to the website and click on 'Subscribe')
- If you have any questions, do get in touch with Central Office (**newphytol@lancaster.ac.uk**; tel +44 1524 592918) or, for a local contact in North America, the USA Office (**newphytol@ornl.gov**; tel 865 576 5261)